Earth and Planetary Science Letters 300 (2010) 11–18

Contents lists available at ScienceDirect

Earth and Planetary Science Letters

journal homepage: www.elsevier.com/locate/epsl

Computer simulations of water interactions with low-coordinated forsterite surface sites: Implications for the origin of water in the inner solar system

H.E. King [a,*], M. Stimpfl [b], P. Deymier [c], M.J. Drake [b], C.R.A. Catlow [d], A. Putnis [a], N.H. de Leeuw [d,*]

[a] Institut für Mineralogie, University of Münster, Corrensstrasse 24, 48149, Münster, Germany
[b] Lunar and Planetary Laboratory, University of Arizona, Tucson AZ 85721, USA
[c] Department of Materials Sciences and Engineering, University of Arizona, Tucson AZ 85721, USA
[d] Department of Chemistry, University College London, 20 Gordon Street, London WC1H 0AH, UK

ARTICLE INFO

Article history:
Accepted 13 October 2010
Available online 29 October 2010

Editor: T. Spohn

Keywords:
planetary accretion
water chemisorption
forsterite
fractal surfaces

ABSTRACT

Adsorption of water to fractal dust grains during accretion has been proposed as a possible source of water for rocky planets. We have used computer simulations to study the feasibility of chemisorption onto forsterite dust grains by investigating the adsorption of dissociated water to stoichiometric and defective surfaces. Defects were modeled using steps, corner sites and vacancies on different forsterite surfaces. Our results show that water dissociation is expected on the stoichiometric (100) surface but not on the stoichiometric (010) surface. However, the energies released by dissociative adsorption at steps and corners indicate that the energetic barrier to chemisorption on the (010) surface would be favorable if these features were present. Steps and corners on all surfaces studied produced Mg sites that have low coordination and thus were highly reactive, favoring the dissociation of water. Terrace size between the steps was shown to have a limited effect on the final energies, although smaller terraces created more reactive Mg sites at corners. A simple Langmuir model was used with the energetic data from our simulations to examine the effectiveness of water adsorption at temperature and pressure conditions applicable to the accretion disk. The findings of this study suggest that water would be strongly chemisorbed at fractal forsterite surfaces even at low partial pressures suggesting that water could be retained during planetary accretion.

1. Introduction

The origin and mechanism of water incorporation into rocky planets, such as the Earth, is not well understood. The three central theories presently used to describe the incorporation of water are based on the origin of the water-bearing material and whether the water was incorporated during or after accretion (Ciesla and Lauretta, 2005; Drake, 2005; Lunine et al., 2003; Morbidelli et al., 2000). In these models comets and asteroids are considered the most plausible sources of water. However, differences between the isotopic signatures of comets and asteroids and those of the Earth indicate that, combined or individually, these sources could not have provided all of the Earth's water. For example, comparison of the Ar/H_2O ratios for the Earth and comets limits the Earth's water budget from this source to less than 15% (Drake and Campins, 2005). Similar arguments can be used to calculate the contributions from asteroids (Lunine et al., 2003), as represented by present day meteorites. Therefore, either the comets and asteroids had a unique chemical composition at the time of accretion or we must assume that they did not provide the bulk of the Earth's water.

Water vapor and atomic hydrogen have been observed at 1 AU around the young stellar object MWC 80 (Eisner, 2007). This observation in conjunction with the presence of refractory minerals, such as forsteritic olivine, in the dust clouds surrounding Young Solar Objects (YSOs) has led to the proposal that adsorption of water to interstellar dust grains could also be a source of water (Muralidharan et al., 2008; Stimpfl et al., 2006). The coalescence of the dust grains during low energy impacts is expected to create fractal particles with irregular surfaces (Blum and Wurm, 2000; Fogel and Leung, 1998; Weidenschilling and Cuzzi, 1999). These irregular surfaces would facilitate water adsorption due to the presence of highly reactive sites. Even the lowest estimates for lifetimes of gas in the accretion disk, 0.1 My (Fegley, 2000), should provide sufficient time for the adsorption of water to occur on the dust grain surfaces. Therefore, if the water can form strong bonds with the surface, i.e. chemisorption, the resulting products would be able to withstand desorption even at high temperatures.

Preliminary investigations of water adsorption on the mineral forsterite have been conducted by Stimpfl et al. (2006) and Muralidharan et al. (2008) using energy minimization and Monte Carlo simulations. Their results show that strong adsorption sites

* Corresponding authors. Tel.: +49 251 83 33456; fax: +49 251 83 38397.
E-mail addresses: hking_01@uni-muenster.de (H.E. King), n.h.deleeuw@ucl.ac.uk (N.H. de Leeuw).

0012-821X/$ – see front matter © 2010 Elsevier B.V. All rights reserved.
doi:10.1016/j.epsl.2010.10.019

are available to the water molecule on the anhydrous surface. Muralidharan et al. (2008) showed that at conditions applicable in the accretion disk between 1 and 3 of the Earth's oceans of water could potentially be adsorbed to the dust grains. However, these studies did not account for the presence of pores, steps or other defects expected on the fractal grain surfaces that would facilitate water sequestration via the formation of strong covalent bonds (chemisorption). To fully examine the feasibility of adsorption at dust grains as a planetary water source, it is necessary to understand the potential of dissociative adsorption as an alternative/concomitant mechanism for retaining water at the surface. Preliminary work by de Leeuw et al. (2010) has shown that chemisorption of water may be feasible at conditions of the accretion disk, but an in-depth study is required to fully examine the feasibility of adsorption at dust grains as a planetary water source. Therefore, we have performed a detailed study of the configurations and energies obtained by adsorption of dissociated water molecules on a range of different perfect and defective forsterite surface sites. Surface defects, including steps, corner sites and vacancies, are expected to be common on the fractal dust grain surfaces, providing under-coordinated surface species and increasing the surface reactivity by destabilizing the surface. The stoichiometric (010) and (100) planar surfaces were chosen because they were studied using associative adsorption by Stimpfl et al. (2006). In addition we created a series of irregular surfaces with different surface features to model the fractal nature of the dust grains. Finally, using a simple Langmuir model we have used the energetic data obtained in our simulations to investigate the effectiveness of the adsorption process at pressure/temperature conditions characteristic of the accretion disk.

2. Methodology

We have used interatomic potential-based (IP) simulation techniques to calculate the geometries and energies of the fractal forsterite surfaces and their interaction with dissociated water. IP methods are based on the Born model of solids (Born and Huang, 1954), which assumes that the ions in the crystal interact via long-range electrostatic forces and short-range forces, including both the repulsions and the van der Waals attractions between neighboring electron charge clouds. The long-range Coulombic interactions in the surface systems are calculated using the Parry technique (Parry, 1975, 1976), which is adapted from the well-known Ewald method for 3-dimensional systems, whereas the short-range forces are described by parameterized analytical expressions. The electronic polarizability of the ions is included via the shell model of Dick and Overhauser (1958) in which each polarizable ion, in our case the oxygen ion, is represented by a core and a massless shell connected by a spring. The polarizability of the model ion is then determined by the spring constant and the shell charge, which are obtained by fitting to experimental dielectric constants when available. In addition, it is often necessary to include angle-dependent forces to allow for partially covalent bonds, for instance in the silicate groups.

The potential parameters used for the simulation of the Mg_2SiO_4 system are a combination of the SiO_2 potential of Sanders et al. (1984) and the MgO potential of Lewis and Catlow (1985). These combined potentials have been used to good effect to model bulk and defect properties of forsterite, (Parker and Price, 1989; Price et al., 1987) and the structures and stabilities of its surfaces and grain boundaries (de Leeuw et al., 2000a,b; Watson et al., 1997). The potential parameters for the dissociated water molecule are taken from Baram and Parker (1996), who have expanded the earlier model of Saul et al. (1985) by including a polarizable oxygen ion. These parameters have been used in simulations of the dissociative adsorption of water at the surfaces of ionic oxides (de Leeuw et al., 1995), silica (Du and de Leeuw, 2004, 2006) and zeolites (Baram and Parker, 1996; Higgins et al., 2002). In addition to these studies, the parameters have been employed previously for the forsterite mineral to investigate full monolayer hydration of a number of planar surfaces and grain boundaries (de Leeuw et al., 2000a,b). The complete potential model used in this work is listed in Table 1.

We have employed energy minimization techniques to investigate the structures and stabilities of the different surface sites and their interaction with dissociated water molecules. We have used the METADISE code (Watson et al., 1996), which is designed specifically to model dislocations, interfaces and surfaces. Following the approach of Tasker (1979), the crystal is described as a series of charged planes parallel to the surface/boundary and periodic in two dimensions; it is then divided into two blocks each comprising two regions, region I and region II. Region I contains those atoms near the extended defect, in this case the surface and adsorbed water, and a few layers immediately below; these atoms are allowed to relax to their mechanical equilibrium. Region II contains those atoms further away, which represent the rest of the crystal and are kept fixed at their bulk equilibrium position. The energies of the blocks are essentially the sum of the energies of interaction between all atoms. It is necessary to include region II to ensure that the total interaction energy of an ion at the bottom of region I is modeled correctly. Each geometry optimization started with a conjugate gradients energy minimization, which was completed when the energy between successive iterations differed by less than 0.05 eV for region I of the surface simulation cell, followed by a Newton Raphson energy minimization with an energy convergion criterion of 10^{-5} eV between successive iterations.

The surface energy (γ) is a measure of the thermodynamic stability of the surface with a low, positive value indicating a stable surface; γ is calculated as follows:

$$\gamma = \frac{E_S - E_B}{A} \quad (1)$$

Table 1
Potential parameters used in our simulations. Two body potentials cut-off at distances beyond 10 Å.

Charges (e)			Core–shell interaction ($eVÅ^{-2}$)
Ions	Core	Shell	
Mg	+2.00000		
Si	+4.00000		
H	+0.40000		
Oxide oxygen (O_{OX})	+0.84819	−2.84819	74.92038
Hydroxide oxygen (O_{OH})	+0.90000	−2.30000	74.92038
Buckingham potential	A (eV)	ρ (Å)	C ($eVÅ^6$)
Mg–O_{OX}	1428.5	0.29453	0
Mg–O_{OH}	941.5	0.29453	0
Si–O_{OX}	1283.90734	0.32052	10.66158
Si–O_{OH}	983.55600	0.32052	10.66158
O_{OX}–O_{OX}	22764.3	0.14900	27.88
O_{OX}–O_{OH}	22764.3	0.14900	13.94
O_{OH}–O_{OH}	22764.3	0.14900	6.97
H–O_{OX}	396.27	0.25000	0
H–O_{OH}	311.97	0.25000	0
Morse potential	D (eV)	α ($Å^{-1}$)	r_0 (Å)
H–O_{OH}	7.052500	3.17490	0.94285
Three-body potential	k ($eV\ rad^{-2}$)		Θ_0
O_{OX}–Si–O_{OX}	2.09724		109.470000
O_{OH}–Si–O_{OH}	2.09724		109.470000
O_{OX}–Si–O_{OH}	2.09724		109.470000

where E_s is the energy of the surface block of the crystal, E_B is the energy of an equal number of atoms of the bulk crystal and A is the surface area. The hydration energy (E_{hydr}) is obtained by comparing the energy of the hydrated surface (E_H) directly with the sum of the energies of the dehydrated surface (E_S) and the self-energy of a water molecule (E_{H_2O}), as follows:

$$E_{hydr} = E_H - (E_S + E_{H_2O}) \quad (2)$$

where we have calculated the hydration energy with respect to gaseous water as this would be the stable phase for water in the inner accretion disk. Although the energies calculated are negative and thus a more negative energy results in a stronger interaction with the surface, for the sake of clarity we will discuss the energies calculated in terms of their absolute values. Therefore, the reported energies in the text are those required to return the dissociated water molecule to the gas phase by removing it from the surface. Water commonly reacts with oxides via a dissociative mechanism, especially if the surface sites are highly under-coordinated as they are at the fractal surfaces considered in this work. The calculation of the energies for dissociative water adsorption requires a value for the energy of the dissociation of a water molecule:

$$H_2O_{(g)} + O^{2-}_{(g)} \rightarrow 2(OH)^-_{(g)} \quad (3)$$

However, this expression requires the second electron affinity of oxygen, which is material-dependent (Harding and Pyper, 1995). To circumvent this difficulty we can use experimental heats of formation for the reaction:

$$Mg_2SiO_{4(s)} + 4H_2O_{(g)} \rightarrow Si(OH)_{4(g)} + 2Mg(OH)_{2(s)} \quad (4)$$

The reaction enthalpy for reaction (4) was measured at -151.7 kJ mol^{-1} (Greenberg, 1957; Iler, 1979; Weast and Astle, 1981) and using this value in a Born Haber cycle with the calculated lattice energies given in Table 2, the energy of dissociation in reaction (3) was evaluated at -784.4 kJ mol^{-1} This value then becomes the effective self-energy of water, E_{H_2O}, which can be used directly in Eq. (2) for a dissociated water molecule. This method of calculating hydration energies for dissociatively adsorbed water has been used for a range of minerals, including MgO (de Leeuw et al., 1995), SiO_2 (de Leeuw et al., 1999) and Mg_2SiO_4 (de Leeuw et al., 2000a,b), where complete monolayer adsorption of water was examined over various forsterite surfaces. Those results showed a good agreement between experimental and calculated crystal morphologies, suggesting that the potential model and the method of calculating hydration energies is sufficiently accurate to reproduce the relative surface stabilities of the hydrated mineral (de Leeuw et al., 2000a).

3. Results and discussion

Forsterite (Mg_2SiO_4) is the Mg end-member of the isomorphic solid solution $(Mg,Fe)_2SiO_4$ generally known as olivine, which has the space group P*bnm*. The bulk structure of olivine is composed of a distorted hexagonally close-packed array of oxygen with 1/8 of the tetrahedral sites occupied by Si^{4+} and 1/2 of the octahedral sites occupied by divalent cations (mainly Mg and Fe). Of the two octahedral sites the M1 site, which is more distorted and smaller than M2, forms edge-sharing chains parallel to the ***c*** axis. We have used the unit cell of a = 4.7560 Å, b = 10.2070 Å and c = 5.9800 Å, $\alpha = \beta = \gamma = 90°$ (Smyth and Hazen, 1973) as our starting structure, which upon energy minimization using the potential model in Table 1, relaxed to a minimum-energy configuration with a = 4.7898, b = 10.2464 Å and c = 5.9863 Å, $\alpha = \beta = \gamma = 90°$ i.e. very close to the experimental values. Figure 1 shows the perfect forsterite structure with the octahedral magnesium sites marked M1 and M2.

When the surfaces were created the SiO_4 units were kept intact, in agreement with previous Density Functional Theory calculations, which have shown that forsterite is primarily an ionic material where the SiO_4 groups act as polyanions (de Leeuw, 2001). We have considered two stoichiometric surfaces, the (010) and (100), and a number of reconstructed dipolar surfaces, which contain Mg and SiO_4 surface vacancies (de Leeuw et al., 2000a). Finally, the fractal surfaces were created from the planar (010), (110) and (101) surfaces by first introducing steps on the surfaces with intervening terraces of increasing areas, as described in de Leeuw et al. (2000b). A second step at right angle to the first was then introduced on one of the (010) stepped surfaces to create surface corner sites at the (010) surface. The resulting surfaces, which are highly irregular with a variety of low-coordinated and hence reactive surface sites, were geometry-optimized before hydration of the different surface sites. A number of optimized surface geometries are shown in Figure 2, with all surface energies listed in Table 3, which clearly shows that the irregular surface structures with high densities of under-coordinated surface species are less stable than more regular, planar surfaces, for example the stoichiometric (010) surface which has a calculated surface energy of $\gamma = 1.28$ Jm^{-2} (de Leeuw et al., 2000a).

3.1. Surface hydration

We first investigated the dissociative adsorption of water molecules at two planar surfaces, the stoichiometric (010) and (001) surfaces. We have used a different procedure from our previous work, where we investigated the surface structures and stabilities of the forsterite minerals at Earth surface conditions (de Leeuw et al., 2000a). Previously, we hydrated bulk-terminated surfaces to full

Table 2
Calculated lattice energies used to calculate the energy released upon the dissociation of one water molecule.

Calculated lattice energies (kJ mol^{-1})	
$MgO_{(s)}$	−3984.8
$Mg(OH)_{2_{(s)}}$	−3378.3
$SiO_{2_{(s)}}$ (quartz)	−12414.0
$Si(OH)_{4_{(g)}}$	−10784.6

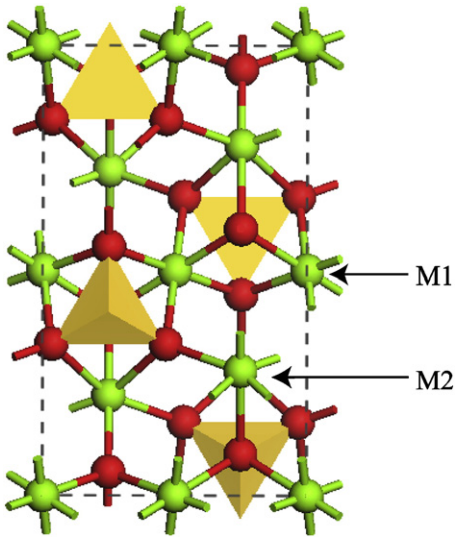

Fig. 1. Perfect forsterite lattice, octahedral Mg sites are labeled M1 and M2. SiO_4 units are represented by yellow tetrahedra, Mg as green spheres and O as red spheres.

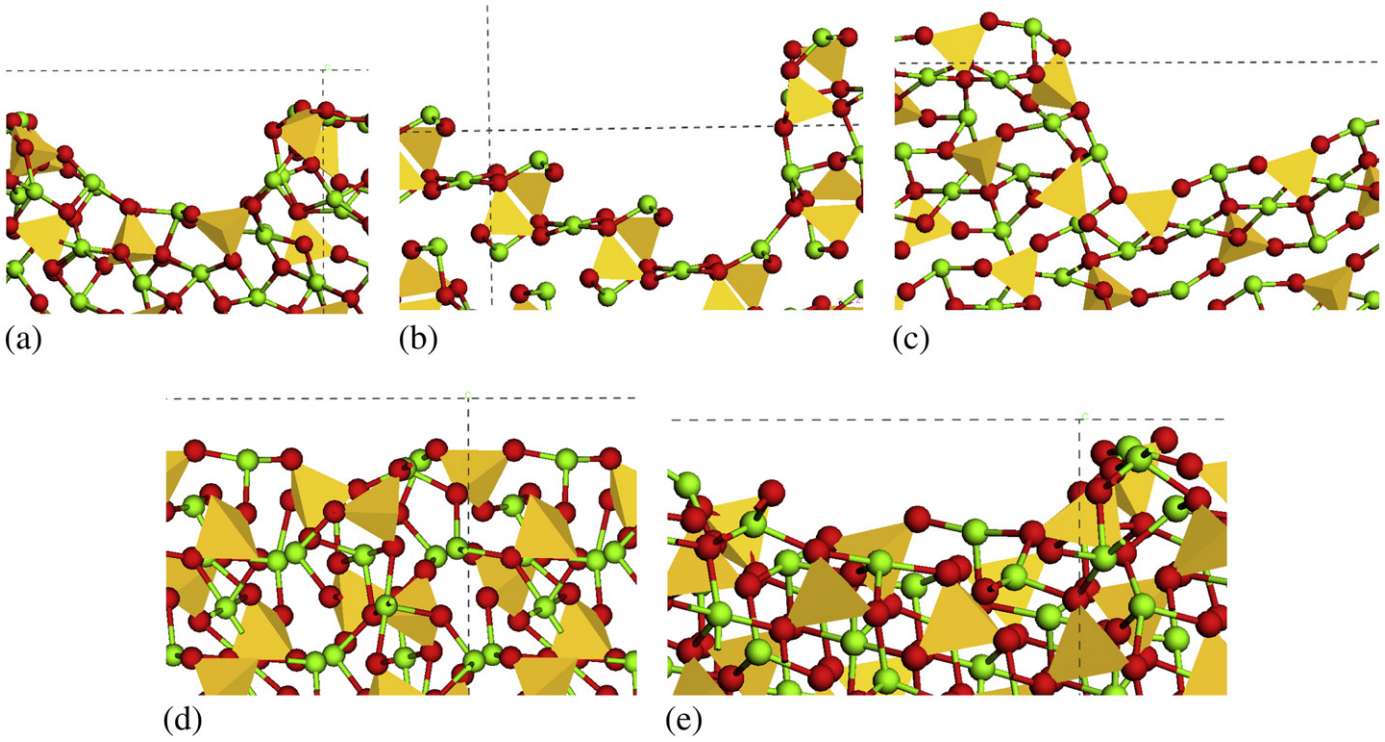

Fig. 2. (a) and (b) Steps in different orientations on the (010) surface. (c) Corner on (010) surface created by cutting the (010) surface perpendicular to the small steps that can be seen in (b), the small steps lie parallel to the plane of the page. (d) Small step created on the (110) surface and (e) step on the (101) surface. (SiO_4 units: yellow tetrahedra, Mg: green spheres, and O: red spheres.)

monolayer coverage before minimization of the entire hydrated surface system, a reasonable protocol as hydration would occur instantaneously once the mineral surface was exposed. However, as the partial pressure of water (p_{H_2O}) in the accretion disk was probably too low (10^{-8} bars), and the temperatures too high (700–1100 K) in the early stages of accretion to allow full monolayer coverage to be obtained, here we have investigated the process of adsorption of a single isolated water molecule to examine the reactivity of forsterite at the surface–vacuum interface, as was done by Stimpfl et al. (2006) for physisorption. Indeed, Muralidharan et al. (2008) have used kinetic Monte Carlo simulations of the associative adsorption of water at forsterite surfaces, a necessary preliminary state to the dissociation of the water molecules, to show that at temperatures of 700 K, we can at best expect a single layer coverage of 15 water molecules/nm^2 that decreases rapidly with increasing temperature. Thus, in the present calculations we have first relaxed the dehydrated surface structures before adsorbing isolated water molecules at the different surface sites. Where required, we have used (2×2) surface supercells to increase the surface area, thus ensuring that each adsorbed water molecule was isolated entirely from its images in neighboring cells, hence providing a more realistic model for the adsorption of water onto accretion disk dust particles.

Table 3
Adsorption energies calculated for each of the surfaces studied and the coverage generated by the adsorption of a single dissociated water molecule.

Surface structure/ orientation	Surface stability (J/m^2)	Fraction of hydrated sites	Dissociative adsorption energy (kJ mol^{-1})	Associative adsorption energy (kJ mol^{-1})
Stoichiometric (010)	1.28	1/3	−79.4	−120.0[d]
Stoichiometric (100)	2.57	1/8	−320.2	−160.0[d]
Dipolar (001)	1.74	1/5	−228.8	−160.7[e]
Dipolar (010)	2.32	1/6	−299.5	−170.4[e]
Dipolar (100)	2.25	1/6	−288.7	−146.2[e]
Stepped (010)[a]	2.34	1/20	−229.6	–
Stepped (010)[b]	2.16	1/14	−246.3	–
Stepped (010)[c]	2.12	1/20	−272.9	–
Stepped (110)	1.88	1/10	−334.2	–
Stepped (101)	1.82	1/25	−185.6	–

[a] Small step.
[b] Large step.
[c] Corner.
[d] Stimpfl et al. (2006).
[e] Data extrapolated from De Leeuw et al. (2000a).

Hydration energies are determined both by the interaction of the water molecule with the surface, as well as by the interactions between adsorbed water molecules, which may stabilize adsorption through the formation of a network of intermolecular hydrogen bonding (Lindan et al., 1997) or destabilize adsorption through steric hindrance between the adsorbed water molecules. For example, on the stoichiometric (010) surface, the adsorption energy per water molecule increases by almost 10 kJ mol^{-1} from 79.4 kJ mol^{-1} to 89.2 kJ mol^{-1} as adsorption increases from an isolated water molecule (0.25 coverage) to full monolayer coverage. In contrast, on the (001) surface full monolayer coverage decreases the individual adsorption energy of the water molecules by more than 100 kJ mol^{-1} (from 228.8 kJ mol^{-1} to 120.6 kJ mol^{-1}) due to unfavorable interactions between the water molecules that do not allow the optimum interaction between the surface and adsorbed water. The strength of adsorption of an isolated water molecule thus may be enhanced or diminished compared to full monolayer coverage, justifying our protocol in this work where the adsorption of isolated, gaseous water molecules at the mineral/vacuum interface needs to be considered.

Under near-vacuum conditions, stoichiometric surfaces will be the most stable and hence we have first calculated the dissociative adsorption of isolated water molecules at the stoichiometric (010) and (100) surfaces, shown in Figure 3, which were considered by Stimpfl et al. (2006) and Muralidharan et al. (2008) for the associative adsorption of water. On the (010) surface, the energy released upon dissociative adsorption of an isolated water molecule is calculated to

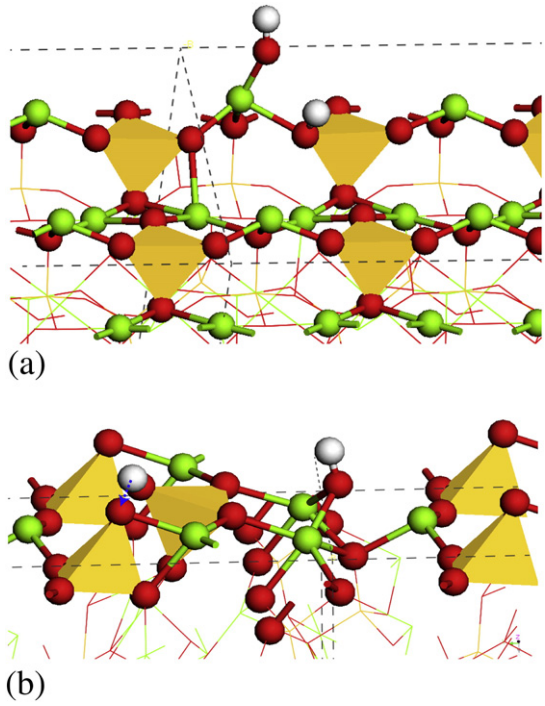

Fig. 3. Adsorption of dissociated water to the stoichiometric planar surfaces. (a) Adsorption to the stoichiometric (010) surface and (b) adsorption to the (100) surface, where the dotted blue arrow represents an H-bond. (SiO_4: yellow tetrahedra, O: red spheres, H: white spheres and Mg: green spheres. Atoms below the surface are represented by lines.)

be 79.4 kJ mol^{-1}. As the hydration energy for associative adsorption of water at this surface is calculated from both interatomic potential simulations and ab initio methods to be significantly larger, approximately 120 kJ mol^{-1} (de Leeuw et al., 2000a; Stimpfl et al., 2006), associative adsorption will not proceed to the dissociation of the water molecule at the surface. The energy released upon dissociative adsorption of an isolated water molecule at the stoichiometric (100) surface, however, is large at 320.2 kJ mol^{-1}. Associative adsorption, releasing up to 160 kJ mol^{-1} at this surface (Stimpfl et al., 2006), should therefore be followed by dissociation of the water molecule at the surface with the formation of strong chemical bonds to surface Mg and O species.

3.2. Adsorption at low-coordinated surface sites

As mentioned earlier, one of the major features distinguishing accretion disk dust particles from mineral crystals found at the Earth's surface is the highly fractal nature of their surfaces, which leads to a large number of under-coordinated surface sites available for water adsorption. Generally, low-coordinated sites are highly reactive. Previous ab initio and interatomic potential-based calculations of water adsorption at low-coordinated sites have shown that dissociative adsorption is commonly preferred over associative adsorption at these sites (de Leeuw and Purton, 2001; de Leeuw et al., 1996). We may therefore expect strong chemisorption of water at the fractal surface sites of forsterite.

For all dipolar and stepped surfaces examined we observe that dissociated water adsorption is thermodynamically stable and results in large adsorption energies. These energies, shown in Table 3, indicate that strong interactions occur between water and the surface. For comparison, Table 3 also lists the energies of associative adsorption at the stoichiometric and dipolar surfaces, obtained from previous work (de Leeuw et al., 2000a; Stimpfl et al., 2006). As mentioned in Section 3.1, associative adsorption of water is clearly preferred on the stoichiometric (010) surface, which is the most stable of the surfaces studied. The preference for weak physisorption of water molecules at the (010) surface is consistent with Density Functional Theory calculations, which showed that water initially adsorbed dissociatively at this surface recombines to form associatively adsorbed water molecules (de Leeuw, 2001). Preferential physisorption of water is also a general phenomenon observed at exceptionally stable mineral surfaces, for example at the CaO (100), alpha-quartz (0001) and fluorite (111) surfaces (de Leeuw and Purton, 2001; de Leeuw et al., 2000c; Du and de Leeuw, 2004). Apart from the stoichiometric (010) surface, dissociative adsorption is preferred at all other forsterite surfaces (Table 3). However, although the energies of adsorption to the steps are large, they are similar to those found for dipolar surfaces and the stoichiometric (100) surface. These results indicate that on highly stable surfaces, e.g. (010) that discourage the dissociation of water, low-coordinated steps and corner sites could provide areas where this process becomes energetically favorable and thus allow water to be chemisorbed. However, steps and corner sites on less stable surfaces could aid adsorption by providing easily accessible sites but would not affect the hydration energy.

The reactivity of different stepped surfaces is governed by various factors, the most important being the presence and location of low-coordinated O atoms on the dehydrated surface and the extent to which the O sites nearest potential Mg surface ions (within 2 Å) are under-coordinated. For the two least reactive stepped surfaces the original surfaces had more three-coordinated O atoms than two-coordinated O atoms available for hydration. In contrast, most of the O sites available for adsorption on the three most reactive stepped surfaces had a coordination number of two making the surfaces more reactive. The location of the most favorable Mg site is dependent on the dehydrated surface features, size of the step and the distance between surface Mg atoms. The OH group from the water molecule is able to interact with two Mg surface atoms and preferably adsorbs to a terrace Mg atom behind the step and an Mg atom at the step edge. This increased the step stability by rearranging the surface so that the less reactive silicate tetrahedra were located at the step edge. Stabilization of the step can also occur via bridging between a step edge Mg site and an Mg atom on the lower terrace but this was not possible on any of our surfaces. For example, even at the small step (5.37 Å) on the (101) surface the OH group favors adsorption to a second Mg just behind the step edge because the distance between the surface Mg on the step face is too great (Fig. 4a). Both the large degree of rearrangement needed to incorporate the dissociated water molecule and the comparatively long Mg–O bonds to the OH group (2.00 and 1.94 Å) have led to this stepped surface being the least reactive of the surfaces studied.

However, the most reactive surface, the (110), is able to form strong interactions with the dissociated water molecule resulting in Mg–O bond lengths of 1.88 and 1.89 Å. After adsorption at this surface the final configuration allows the Mg ions to become coordinated to four and five O atoms respectively rather than three O atoms on the initial surface. This was the largest increase of Mg–O interactions due to adsorption produced during our simulations. The step on the free surface is small (3.31 Å) and all surface O atoms are under-coordinated and thus available for chemisorption, thereby greatly increasing the probability that a water molecule can stabilize the surface and the step. The (110) surface is also the only surface studied where the original surface contained only three-coordinated Mg atoms. Thus, the step in this example does not create specific under-coordinated sites, but provides easily accessible sites for adsorption.

Terrace size can also affect the surface stability and adsorption energies. We have examined four different terrace areas on the (010) surface with a large step (Fig. 2b). Unexpectedly, on this surface the most energetically preferred configuration was found on the most stable surface, i.e. the surface with the largest terrace. Closer

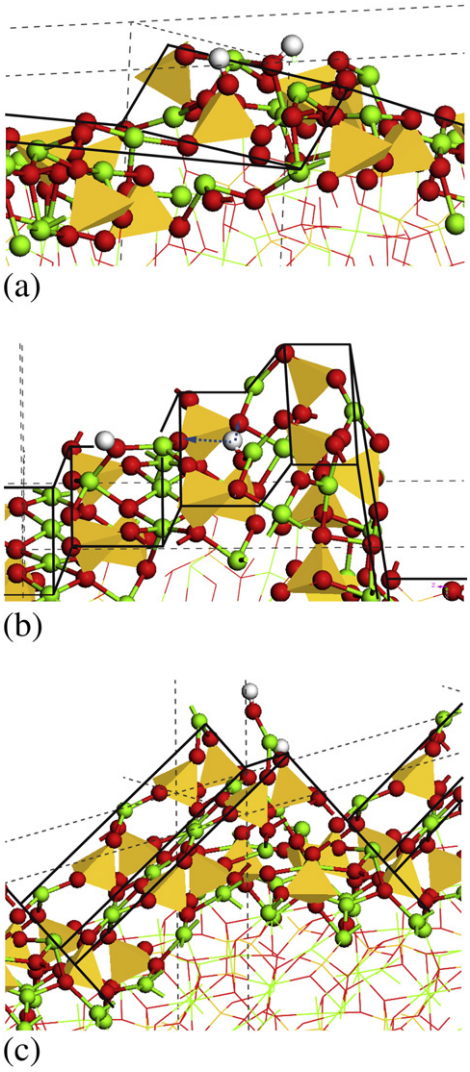

Fig. 4. Examples of the most favorable configurations of dissociated water adsorbed to different defective surfaces. (a) Adsorption to the step on the (101) surface, (b) adsorption of water bridges the smaller steps on the large terrace area of the (010) surface, where the dotted blue arrows represent H-bonds and (c) adsorption to the corner site on the (010) surface. (H: white spheres, Mg: green spheres, O: red spheres and Si: yellow tetrahedra. Atoms situated below the surface are depicted as colored lines, surface contour is highlighted by thick black lines.)

examination reveals that the preferred adsorption site is independent of the original surface stability and is located in different regions of the surface depending on the ability of the surface to relax. On this surface the step is large (8.90 Å) and hence unable to be effectively stabilized by water adsorption, but the terrace has many small steps (2.37 Å) that can be bridged by the OH group adsorbed to Mg sites at the step edges (Fig. 4b). The small steps are located just behind the large step on the surface and adsorption stabilized the large step edge as well as the small steps by rearrangement of the surface atoms to accommodate the water molecule. This surface is unique in these simulations as it is the only example in which H-bonds are formed during adsorption to all the Mg sites examined. In addition to the stabilizing effect of water adsorption, the ability of the OH group to form two H-bonds also helped to stabilize the structure and smooth the surface.

We have studied the effects of corners on the (010) surface by cutting the surface almost perpendicular to the small step (3.10 Å) creating a corner site at the step edge (Fig. 2c, where the large step is 7.81 Å). The corner provides a very favorable site for adsorption and resulted in the only example where the largest hydration energy corresponds to adsorption to just one surface Mg, located at the corner itself (Fig. 4c). This changed the Mg coordination environment from only two O atoms on the dehydrated surface, the lowest number of any of the adsorption sites studied, to three O atoms. The absence of neighboring surface Mg atoms at the corner prevented the formation of additional OH–Mg interactions observed on the other stepped surfaces. However, the stabilization of the surface gained by the effective termination of the corner by the adsorption of an OH group resulted in this site having the largest adsorption energy for this surface (272.9 kJ mol^{-1}). We have also explored the effect of changing the terrace size on the corner site. In contrast to the stepped surfaces, the most favored site is always located at the corner. In these simulations the difference in the final energies is dependent on the initial coordination of the Mg site. The adsorption energies at the three smallest terrace sizes are all similar (268.1 kJ mol^{-1}, 272.9 kJ mol^{-1} and 270.4 kJ mol^{-1} consecutively from the smallest terrace). However, the largest terrace size produced an adsorption energy of 205.4 kJ mol^{-1}. Simulations of the three smallest terraces produced very similar final configurations, either with the H adsorbed to a surface O site that is connected to the OH-bearing Mg, or with the H further away from the Mg site, forming an H-bond with the surface. In all these examples, the corner Mg site was able to increase its interactions after adsorption from two to three O atoms. The Mg corner site on the largest terrace does not change its coordination number because interaction with the water molecule forces the surface to rearrange so that in the final configuration the corner Mg remains coordinated to three O atoms. As a result, less energy is released upon adsorption than at the smaller terraces with lower-coordinated Mg sites at the corners.

In summary, the large energies released upon adsorption to specific sites at defective surfaces are primarily due to the stabilization of under-coordinated Mg atoms, where corners in particular produce highly reactive adsorption sites. The overall affinity of a surface to adsorb a dissociated water molecule is related to the different coordinations of O atoms exposed at the surface. On some of the stepped surfaces the OH group can interact with two surface Mg ions aiding surface stabilization. Comparison of the adsorption energies of the low-coordinated surface sites with energies found for planar stoichiometric surfaces indicates that even stable surfaces may be able to promote the dissociative adsorption of water when steps and corners are present.

3.3. Adsorption as a function of temperature and water partial pressure

The magnitude of the energies associated with water adsorption obtained in this work suggests that the surfaces may also be able to retain water at conditions applicable to the accretion disk.

To test this hypothesis we have determined the partial pressure of gaseous water required to retain water at temperatures expected in the accretion disk, where the adsorption processes at the surface are represented in Eq. (5).

$$Surface + H_2O_{(g)} \overset{K}{\longleftrightarrow} Surface \cdot (H_2O) \tag{5}$$

In this expression K is the equilibrium constant for reaction (5) and *Surface* and *Surface* · (H_2O) represent the mineral surface before and after water adsorption respectively. The equilibrium constant K can be calculated from the Gibbs free energy (G) of adsorption using Eq. (6), where $a_{(s)}$ is the activity of the water molecule adsorbed at the solid surface and $a_{(g)}$ is the water molecule activity in its gaseous state. To calculate the partial pressure of gaseous water ($p_{H_2O(g)}$) at a specific temperature we have used a simple Langmuir model where the partially hydrated surface is represented as $x/(1-x)$, the fraction of surface sites occupied by water is denoted as x, R is the gas constant

and T is a chosen temperature appropriate for accretion disk conditions.

$$K = \frac{a_{(s)}}{a_{(g)}a_{surface}} = \frac{x}{(1-x)p_{H_2O_{(g)}}} = e^{-\Delta G^0/RT} \quad (6)$$

As mentioned previously, the adsorption of a complete water monolayer is not expected in the accretion disk because of low gaseous water partial pressure (10^{-8} bars, Lodders, 2003). Therefore, we consider the adsorption of an isolated water molecule to the most energetically favored surface site. The fractional occupancy (x) is determined from the number of accessible surface sites in each simulation cell that would be occupied if a full water layer was present. Eq. (7) was used to calculate the change in the standard Gibbs free energies for water adsorption at the forsterite surface using the enthalpies and entropies at the required temperatures, where ΔH is the enthalpy of the adsorption process per water molecule, T is the temperature of interest and ΔS is the change in entropy.

$$\Delta G = \Delta H - T\Delta S \quad (7)$$

The enthalpies for the hydration of forsterite surfaces are shown in Table 3 and are obtained directly from our simulations. The entropies of the gaseous water molecule (Table 4) have been taken from the experimental entropies for temperatures between 400 and 1500 K (Lide, 2000).

Two assumptions were made to calculate the Gibbs free energies of the adsorption processes. Firstly, we assume that the adsorption of a water molecule to the surface does not have a large effect on the forsterite entropy, thus only the change in entropy due to the loss of the free water molecule from the gaseous state onto the surface adsorption site needs to be accounted for. The assumption that the entropy of the mineral surface remains largely unchanged when a small molecule is adsorbed at the surface, has already been used in entropy calculations of the adsorption and desorption of $Si(OH)_4$ species from quartz surfaces, where the calculated trends were shown to be in good agreement with experiment (Du and de Leeuw, 2004). Secondly, we assume that the enthalpies of the adsorption processes, which are calculated without taking into account the temperature of the system, will not be significantly affected by temperature (other than the entropy change in the water molecule). As the hydration enthalpies are lattice energy differences rather than absolute values, we consider this to be a reasonable approximation and one which we have made before in our calculations of the adsorption of water at iron (hydr)oxide surfaces (de Leeuw and Cooper, 2007). Using these two approximations we have calculated the Gibbs free energies for the water adsorption as in Eq. (7). From these calculated Gibbs free energies at temperatures applicable to the accretion disk, we determined the gaseous water partial pressures required for adsorption to occur using Eq. (6).

Table 4
Entropies of gaseous water.

Temperature (K)	S ($JK^{-1}\,mol^{-1}$ at 1 bar)[a]	TΔS ($kJ\,mol^{-1}$)
273.15	0	0
298.15	188.832	−56.3
400	198.791	−79.5
500	206.542	−103.3
600	213.067	−127.8
700	218.762	−153.1
800	223.858	−179.1
900	228.501	−205.7
1000	232.792	−232.8
1100	236.797	−260.5
1200	240.565	−288.7
1300	244.129	−317.4
1400	247.516	−346.5
1500	250.745	−376.1

[a] Values taken from Lide, 2000.

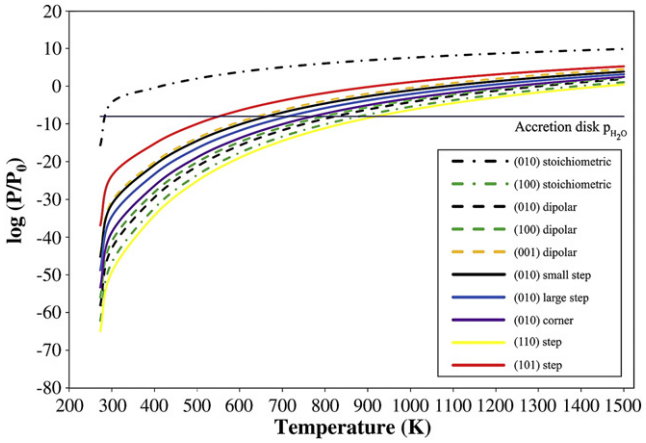

Fig. 5. Partial pressures required to obtain modeled dissociative adsorption coverage on the different surfaces at temperatures expected in the accretion disk. The partial gas pressure of water in the accretion disk (p_{H_2O}) is taken from Lodders (2003).

Figure 5 shows the partial pressure versus temperature plots for the dissociative adsorption of water to the different surfaces examined in this study (listed in Table 3). The plot shows that at the most reactive surface sites, provided by the steps and particularly corner sites on the (010) surface, the adsorption of water could occur up to approximately 1000 K at the low partial pressures of gaseous water of around 10^{-8} bars (Lodders, 2003) as were prevalent in the early accretion disk. Thus, it would appear from these calculations that even at the relatively high temperatures of 500–1500 K (Boss, 1998) and low partial water pressures during the initial stages of planet accretion, fractal forsterite dust grains should be able to retain chemisorbed water at their surfaces.

4. Conclusions

In all the simulations studied, the system 'surface plus water' was energetically preferred over the anhydrous surface, although the strength of adsorption of the dissociated water molecule is highly dependent on the coordination of the surface site and the final geometry. The planar stoichiometric (010) surface is not expected to promote the dissociation of water because the energies found in this study are lower than those in Stimpfl et al. (2006) for the associative adsorption of water. However, on the less stable (100) surface we would expect dissociative chemisorption to follow physisorption because all of the available surface sites release hydration energies for dissociative adsorption that are larger than their counterparts for associative adsorption. This would form the type of strong interaction with the surface that is required for water retention during planetary accretion.

The introduction of steps and corners as surface defects has shown that on stable surfaces, such as the (010) surface, the energies of dissociative adsorption of water are increased markedly. However, on less stable surfaces where the dissociation of water is already expected to occur, the presence of steps has no significant effect on the hydration energies. It is the presence of low-coordinated surface sites, whether located at step edges or corners or on terraces, which determines the strength of the interaction with the water molecules.

By using a simple Langmuir adsorption model, we have shown that even at the low partial pressures of gaseous water and high temperatures expected in the accretion disk retention of water at forsterite surfaces is thermodynamically possible. Thus, these findings strengthen the argument that adsorption to dust grains in the accretion disk could be a viable source of water for rocky planets.

Given that Muralidharan et al. (2008) find that 1–3 Earth oceans of water could be adsorbed by associative adsorption onto perfect forsterite surfaces, this work suggests that substantially more Earth oceans of water were adsorbed prior to planetary accretion onto the building blocks of the terrestrial planets, including the Earth.

Acknowledgements

This research was funded by the European Commission through the EU Research Training Network MIN-GRO Contract no. MRTN-CT-2006-035488. MJD and MS would like to acknowledge support from NASA grant number 'NAG 12795' and MS and NHdL thank the Royal Society for funding an International Incoming Short Visit by MS to University College London.

References

Baram, P.S., Parker, S.C., 1996. Atomistic simulations of hydroxide ions in inorganic solids. Philos. Mag. B 73, 49–58.
Blum, J., Wurm, G., 2000. Experiments on sticking, restructuring, and fragmentation of preplanetary dust aggregates. Icarus 143, 138–146.
Born, M., Huang, K., 1954. Dynamical Theory of Crystal Lattices. Oxford University Press, Oxford.
Boss, A.P., 1998. Temperatures in protoplanetary disks. Annu. Rev. Earth Planet. Sci. 26, 53–80.
Ciesla, F., Lauretta, D., 2005. Radial migration and dehydration of phyllosilicates in the solar nebula. Earth Planet. Sci. Lett. 231, 1–8.
de Leeuw, N.H., 2001. Density functional theory calculations of hydrogen-containing defects in forsterite, periclase, and α-quartz. J. Phys. Chem. B 105, 9747–9754.
de Leeuw, N.H., Cooper, T.G., 2007. Surface simulation studies of the hydration of white rust $Fe(OH)_2$, goethite a-FeO(OH) and hematite a-Fe_2O_3. Geochim. Cosmochim. Acta 71, 1655–1673.
de Leeuw, N.H., Purton, J.A., 2001. Density-functional theory calculations of the interaction of protons and water with low-coordinated surface sites of calcium oxide. Phys. Rev. B 63, 195417.
de Leeuw, N.H., Watson, G.W., Parker, S.C., 1995. Atomistic simulations of the effect of dissociative adsorption of water on the surface structure and stability of calcium and magnesium oxide. J. Phys. Chem. 99, 17219–17225.
de Leeuw, N.H., Watson, G.W., Parker, S.C., 1996. Atomistic simulation of adsorption of water on three-, four- and five-coordinated surface sites of magnesium oxide. J. Chem. Soc., Faraday Trans. 92, 2081–2091.
de Leeuw, N.H., Higgins, F.M., Parker, S.C., 1999. Modeling the surface structure and stability of α-quartz. J. Phys. Chem. B 103, 1270–1277.
de Leeuw, N.H., Parker, S.C., Catlow, C.R.A., Price, G.D., 2000a. Modelling the effect of water on the surface structure and stability of forsterite. Phys. Chem. Miner. 27, 332–341.
de Leeuw, N.H., Parker, S.C., Catlow, C.R.A., Price, G.D., 2000b. Proton-containing defects at forsterite {010} tilt grain boundaries and stepped surfaces. Am. Mineral. 85, 1143–1154.
de Leeuw, N.H., Purton, J.A., Parker, S.C., Watson, G.W., Kresse, G., 2000c. Density functional theory calculations of adsorption of water at calcium oxide and calcium fluoride surfaces. Surf. Sci. 452, 9–19.
de Leeuw, N.H., Catlow, C.R.A., King, H.E., Putnis, A., Muralidharan, K., Deymier, P., Stimpfl, M., Drake, M.J., 2010. Where on Earth has our water come from? Chem. Commun. doi:10.1039/c0cc02312d.
Dick, B.G., Overhauser, A.W., 1958. Theory of the dielectric constants of alkali halide crystals. Phys. Rev. 112, 90–103.
Drake, M.J., 2005. Origin of water in the terrestrial planets. Meteorit. Planet. Sci. 40, 519–527.
Drake, M.J., Campins, H., 2005. Origin of water on the terrestrial planets. Asteroid, Comets, Meteors, Proceedings IAU Symposium No 229, pp. 381–394.
Du, Z.M., de Leeuw, N.H., 2006. Molecular dynamics simulations of hydration, dissolution and nucleation processes at the α-quartz (0001) surface in liquid water. Dalton Trans. 2623–2634.
Du, Z.M., de Leeuw, N.H., 2004. A combined density functional theory and interatomic potential-based simulation study of the hydration of nano-particulate silicate surfaces. Surf. Sci. 554, 193–210.
Eisner, J.A., 2007. Water vapour and hydrogen in the terrestrial-planet-forming region of a protoplanetary disk. Nature 447, 562–564.
Fegley Jr., B., 2000. Kinetics of gas–grain reactions in the solar nebula. Space Sci. Rev. 92, 177–200.
Fogel, M.E., Leung, C.M., 1998. Modeling extinction and infrared emission from fractal dust grains: fractal dimension as a shape parameter. Astrophys. J. 501, 175–191.
Greenberg, S.A., 1957. Thermodynamic functions for the solution of silica in water. J. Phys. Chem. 61, 196–197.
Harding, J.H., Pyper, N.C., 1995. The meaning of the oxygen second-electron affinity and oxide potential models. Philos. Mag. Lett. 71, 113–121.
Higgins, F.M., de Leeuw, N.H., Parker, S.C., 2002. Modelling the effect of water on cation exchange in zeolite A. J. Mater. Chem. 12, 124–131.
Iler, R.K., 1979. The Chemistry of Silica; Solubility, Polymerization, Colloid and Surface Properties, and Biochemistry. John Wiley, New York.
Lewis, G.V., Catlow, C.R.A., 1985. Potential models for ionic oxides. J. Phys. C: Solid State Phys. 18, 1149–1161.
Lide, D.R., 2000. CRC Handbook of Chemistry and Physics, 81st ed. CRC Press, Boca Raton.
Lindan, P.J.D., Muscat, J., Bates, S., Harrison, N.M., Gillan, M., 1997. Ab initio simulation of molecular processes on oxide surfaces. Faraday Discuss. 106, 135–154.
Lodders, K., 2003. Solar system abundances and condensation temperatures of the elements. Astrophys. J. 591, 1220–1247.
Lunine, J.I., Chambers, J., Morbidelli, A., Leshin, L.A., 2003. The origin of water on Mars. Icarus 165, 1–8.
Morbidelli, A., Chambers, J., Lunine, J.I., Petit, J.M., Robert, F., Valsecchi, G.B., Cyr, K.E., 2000. Source regions and timescales for the delivery of water to the Earth. Meteorit. Planet. Sci. 35, 1309–1320.
Muralidharan, K., Deymier, P., Stimpfl, M., de Leeuw, N.H., Drake, M.J., 2008. Origin of water in the inner solar system: a kinetic Monte Carlo study of water adsorption on forsterite. Icarus 198, 400–407.
Parker, S.C., Price, G.D., 1989. Computer modelling of phase transitions in minerals. Adv. Solid State Chem. 1, 295–327.
Parry, D.E., 1975. The electrostatic potential in surface region of an ionic crystal. Surf. Sci. 49, 433–440.
Parry, D.E., 1976. Errata: the electrostatic potential in the surface region of an ionic crystal. Surf. Sci. 54, 195.
Price, G.D., Parker, S.C., Leslie, M., 1987. The lattice-dynamics of forsterite. Mineral. Mag. 51, 157–170.
Sanders, M.J., Leslie, M., Catlow, C.R.A., 1984. Interatomic potentials for SiO_2. J. Chem. Soc. Chem. Commun. 1271–1273.
Saul, P., Catlow, C.R.A., Kendrick, J., 1985. Theoretical studies of protons in sodium hydroxide. Philos. Mag. B 51, 107–117.
Smyth, J.R., Hazen, R.M., 1973. The crystal-structures of forsterite and hortonolite at several temperatures up to 900 °C. Am. Mineral. 58, 588–593.
Stimpfl, M., Walker, A.M., Drake, M.J., de Leeuw, N.H., Deymier, P., 2006. An ångström-sized window on the origin of water in the inner solar system: atomistic simulation of adsorption of water on olivine. J. Cryst. Growth 294, 83–95.
Tasker, P.W., 1979. The surface energies, surface tensions and surface structure of the alkalihalide crystals. Philos. Mag. A 39, 119–136.
Watson, G.W., Kelsey, E.T., de Leeuw, N.H., Harris, D.J., Parker, S.C., 1996. Atomistic simulation of dislocations, surfaces and interfaces in MgO. J. Chem. Soc. Faraday Trans. 92, 433–438.
Watson, G.W., Oliver, P.M., Parker, S.C., 1997. Computer simulation of the structure and stability of forsterite surfaces. Phys. Chem. Miner. 25, 70–78.
Weast, R.C., Astle, M.J., 1981. CRC Handbook of Chemistry and Physics, 61st ed. CRC Press, Boca Raton.
Weidenschilling, S.J., Cuzzi, J.N., 1999. Protostar and Planets. University of Arizona Press, Tuscon.